Earth and Planetary Science Letters 584 (2022) 117411

Contents lists available at ScienceDirect

Earth and Planetary Science Letters

www.elsevier.com/locate/epsl

A quantitative framework for global variations in arc geochemistry

Stephen J. Turner [a,*], Charles H. Langmuir [b]

[a] Department of Geosciences, University of Massachusetts, Amherst, MA 01003, United States of America
[b] Department of Earth and Planetary Sciences, Harvard University, Cambridge, MA 02138, United States of America

ARTICLE INFO

Article history:
Received 12 July 2021
Received in revised form 17 January 2022
Accepted 31 January 2022
Available online xxxx
Editor: R. Dasgupta

Keywords:
quantitative modeling
subduction
arc geochemistry

ABSTRACT

Arc magmas are generated by partial melting of a mantle wedge modified by inputs from subducting sediment and igneous ocean crust. Despite this uniform tectonic process, global arc-front stratovolcano compositions exhibit trace element abundances that can vary by more than an order of magnitude. All incompatible elements correlate well, including those that are thought to be wedge derived, "fluid-mobile", and sediment derived. It has been suggested that global variations in arc trace element abundances occur due to the addition of variable slab components to a depleted mantle wedge, though quantitative global models that include both trace elements and isotopes have been lacking. Here we present an alternative framework in which a relatively constant proportion of slab material, consisting of melts both of altered ocean crust and sediment, is added to ambient mantle wedge that varies from more depleted than MORB to as enriched as "EM1" ocean island basalt sources. The modified mantle melts to varying extents, with melting controlled primarily by the thickness of the overlying lithosphere. Thick lithosphere leads to lower extents of melting in the garnet stability field in most continental arcs. Continental arcs also have enriched ambient mantle, likely because of contributions from enriched sub-continental lithospheric mantle. High degrees of melting of more depleted sources cause oceanic arcs to have low incompatible element abundances. Quantitative modeling of these processes shows that this framework can account for the global arc systematics exhibited by arc-front stratovolcanoes and provides a tool to examine regional variations and more unusual magma compositions. Variations in slab temperature and amount of slab input remain important for second-order variations and certain element ratios.

1. Introduction

Studies of subduction zones generally agree that convergent margin volcanism occurs when hydrated crust and sediment subduct and deliver volatile-bearing components to the mantle wedge, lower the solidus, and cause melting (e.g., Kay, 1980; Gill, 1981; Ellam and Hawkesworth, 1988; Miller et al., 1992; Stolper and Newman, 1994; Elliott et al., 1997; Class et al., 2000). There is also a general consensus that the characteristic incompatible trace element patterns of arc magmas (Fig. 1), such as enrichment of Cs, Rb, K, Ba, Th, U, Pb, and Sr relative to the rare-earth elements (REE), and depletion in Nb and Ta, arise because the volatile-bearing components leave behind residual phases when they separate from the slab (Johnson and Plank, 2000; Klimm et al., 2008; Hermann and Rubatto, 2009; Skora and Blundy, 2010; Carter et al., 2015; Sisson and Kelemen, 2018).

While there is agreement on this general framework, arc magma compositions vary significantly (Fig. 1) on global (Plank and Langmuir, 1988; Turner and Langmuir, 2015a; Farner and Lee, 2017; Schmidt and Jagoutz, 2017), and regional scales (Carr et al., 1990; Elliott et al., 1997; Patino et al., 2000; Yogodzinski et al., 2017; Turner et al., 2017), between adjacent volcanoes of a single arc (Miller et al., 1992; Martin et al., 2011), and even within individual eruptions (Dungan et al., 2001). A wide range of models have been proposed to account for this diversity. These include variations in crustal processing (e.g., Farner and Lee, 2017), slab diapirism (Marschall and Schumacher, 2012), slab temperature (Plank et al., 2009; Schmidt and Jagoutz, 2017), partial melting (Plank and Langmuir, 1988; Tormey et al., 1991; Turner and Langmuir, 2015b), interactions between slab melts and the mantle wedge (Kelemen et al., 2003; Yogodzinski et al., 2017), variations in water flux (Eiler et al., 2005) and preexisting mantle heterogeneity (Morris and Hart, 1983; Pearce, 1983; Ellam and Hawkesworth, 1988; Woodhead et al., 1993, 2012; Turner et al., 2017).

There have been many attempts to explain this compositional diversity, but most involve only verbal descriptions of conceptual

* Corresponding author.
E-mail address: stephenjudsonturner@gmail.com (S.J. Turner).

https://doi.org/10.1016/j.epsl.2022.117411
0012-821X/

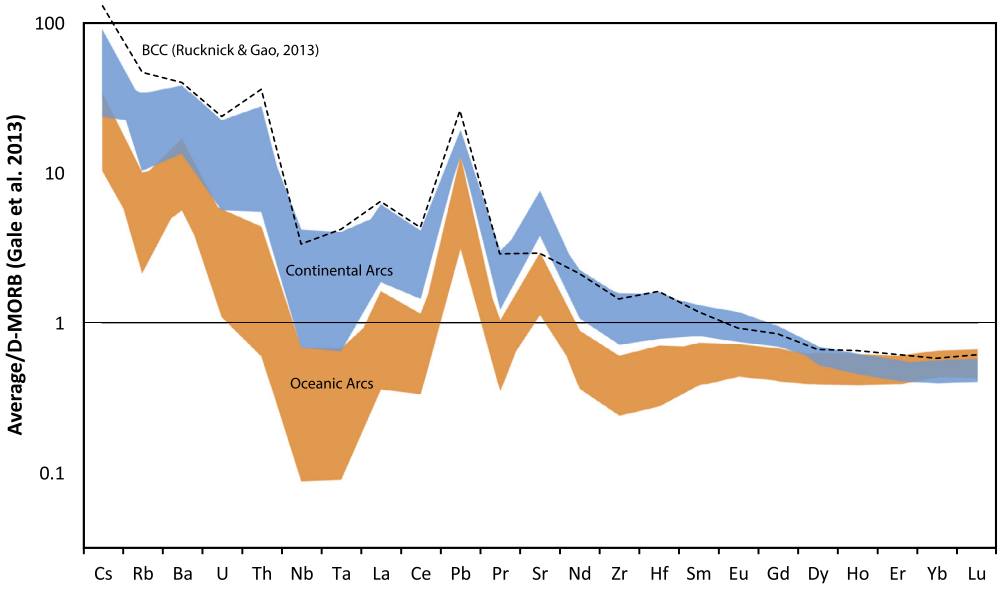

Fig. 1. Summary of global variations among high-Mg# samples (as compiled by Turner and Langmuir, 2022a) from continental arcs with thick crust as compared to oceanic arcs with thin crust. Continental arc volcanoes have much higher abundances of incompatible elements and less prominent "anomalies." Fields are based on the ranges seen among arc segment averages for oceanic arcs and volcano averages for continental arcs, where fewer high-Mg# samples are available (the Central Andes were excluded entirely due to a scarcity of appropriate data). Data in this compilation have Eu/Eu^{*} >0.9 and Mg# from ~55 to ~70. Because the compositional offsets present in this data persist to Mg# ~70 (see Fig. 3), it is implausible that it was produced by intra-crustal processes. We note, however, that there are some atypical cases in which larger compositional swings are found among intermediate-Mg# samples with Mg#~55, though in these cases there is also independent evidence for early crustal contamination (e.g., Davidson and Harmon, 1989; Bezard et al., 2014; Handley et al., 2014). Because our goal is to develop a quantitative framework for parental arc magma variability, samples that have been independently identified as cases of atypical early crustal assimilation have been excluded from the compilation. Detailed descriptions of the qualitative chemical systematics of this dataset, and an extended justification for its use as a representative global sample set for parental arc-front stratovolcanoes can be found in Turner and Langmuir (2022a).

models (e.g., Plank and Langmuir, 1988; Kelemen et al., 2003), diagrams with mixing lines (e.g., Elliott et al., 1997) or quantitative modeling of a small set of elements (e.g., Miller et al., 1992; Freymuth et al., 2016). Others have dealt quantitatively with aspects of data within a single arc (e.g., Yogodzinski et al., 2017; Freymuth et al., 2016; Eiler et al., 2005), but have not tested whether their models are applicable to global-scale observations. Kimura (2017) offers a complex model to calculate subduction zone geochemistry with potential broad applicability, but only provides examples for samples from Japan. Schmidt and Jagoutz (2017) do consider global data and discuss general conclusions from phase equilibria constraints, but do not quantitatively model most trace element abundances or consider isotopic variations. Their study minimizes the important role of variations in ambient mantle composition (e.g., Pearce, 1983) and extent of melting (Plank and Langmuir, 1988; Turner et al., 2016), and includes fore-arc and rear-arc samples of diverse ages that cannot be directly related to constraints from subduction parameters such as lithospheric thickness or convergence rate (see Turner and Langmuir, 2022a). Both Kimura (2017) and Schmidt and Jagoutz (2017) propose that the contrast between slab fluids and slab melts plays a central role in generating global arc magma diversity, but this model conflicts with several key observations of global arc magma compositional systematics (Turner et al., 2016; Turner and Langmuir, 2022a).

A comprehensive understanding of arc volcanism needs to account quantitatively for both intra- and inter-arc geochemical diversity, and the fact that highly incompatible element abundances of arc-front stratovolcanoes vary by up to an order of magnitude, even among high-Mg# samples (Turner and Langmuir, 2015a). Here, we present an internally consistent, quantitative framework that accounts for the trace element and radiogenic isotope characteristics of the arc-front stratovolcanoes that are the predominant manifestation of subduction volcanism. We make use of rear-arc volcanism to constrain the mantle wedge composition, but do not otherwise deal with across-arc variations. In a companion paper (Turner and Langmuir, in preparation) we demonstrate how this framework can be applied to explain regional variations within individual arcs such as the Marianas and Central America.

Key aspects of this framework include:

- Both sedimentary and basaltic ocean crust layers of the slab melt at the base of the mantle wedge, in agreement with Kelemen et al. (2003). These hydrous slab melts cause flux melting of the overlying wedge.
- Slab melts are added to a mantle wedge that varies from enriched to depleted prior to interacting with the slab component, and this initial (ambient) wedge composition strongly influences certain element and isotope ratios, including many element ratios that are usually attributed to the slab component.
- "Flux melting" occurs in response to water added from the slab, but extents of melting beneath the arc front are not usually controlled by the bulk water contents of the mantle source. While regional variations in source water content are important for rear-arc volcanics (Stolper and Newman, 1994; Kelley et al., 2006; Langmuir et al., 2006), extents of mantle melting beneath the arc front vary mostly due to variations in the thermal structure of the mantle wedge that are driven by the variable thickness of the overlying lithosphere and the slab descent rate.
- Slab temperature variations are not a dominant control on arc elemental abundances, apart from a few unusual tectonic settings (Turner et al., 2016; Turner and Langmuir, 2022a). Varying slab temperatures remain significant but generally have second-order effects relegated to certain element ratios, though the ambient mantle and/or sediment compositions also have a large impact on these ratios.
- Variable sediment compositions contribute both to geochemical diversity within individual arcs and global differences among arc averages. Variations in sediment compositions in

conjunction with a quantitative model of ambient mantle variation can explain global and regional trends in ratios such as Ba/Th that have historically been attributed to slab fluids. Varying slab temperatures generally have a second-order effects on these ratios.

Many of these aspects are not new. The suggestions that extent of melting varies with upper plate structure, that ambient mantle wedge composition varies from enriched to depleted, and that the ocean crust melts, are well known. However, while these ideas have been frequently published, they are not widely accepted. For example, the global study of Kelemen et al. (2003) highlighted evidence for slab melting but did not account for evidence requiring ambient mantle wedge heterogeneity and variations in extent of melting of the mantle. Schmidt and Jagoutz (2017)'s representation of the global systematics of arc geochemistry asserts a universally depleted mantle wedge and large extents of melting and suggests that the ocean crust normally does not melt. The framework presented here accounts for the unresolved issues with models that emphasize slab temperature variations or invoke a central role for element transport to the wedge via "aqueous fluids" and incorporates a wide range of experimental constraints to produce a quantitative geochemical model consistent with the global range of arc magma trace element and isotope compositions.

2. Chemical systematics of arc-front stratovolcano parental magmas

A successful model of subduction-related volcanism needs to account for the first-order global geochemical variability of arc volcanics (Fig. 1) as well as the salient correlations between compositional and tectonic subduction parameters (e.g., Fig. 2). The dataset used here to highlight these key observations was compiled by Turner and Langmuir (2022a), and consists of "high-Mg#" samples from arc-front stratovolcanoes that have compositions consistent with the predominant trends of their volcanic edifice, excluding samples from locations with additional tectonic complexity such as the intra-arc rifting region of the southern Cascades, which is associated with the eruption of depleted "low-K tholeiites" in a continental arc (Conrey et al., 1997), or subduction of fracture zones, slab edge, plateaus, or hotspot tracks, as in Costa Rica and Panama, which produced trace-element enriched magmas in an arc with relatively thin crust (Gazel et al., 2015).

Normalizing arc lava compositions to mid-ocean ridge basalt (MORB), as in Fig. 1, highlights the geochemical impacts of subduction relative to ocean ridge volcanism. From this normalized data, is it clear that continental arcs built on thick crust are more enriched in the most incompatible elements than those from extensional oceanic arcs with thin crust and back-arc spreading centers. The light rare-earth element (LREE) abundances in continental arc volcanoes reach values that are nearly an order of magnitude higher than MORB, while most oceanic arc volcanoes have lower LREE abundances than MORB. The heavy rare earth elements (HREE), on the other hand, are universally depleted relative to MORB and overlap in oceanic and continental arcs. All arc volcanics have higher abundances of Cs, Rb, Ba, U, Th, Pb, and Sr than MORB (Fig. 1). These elements also exhibit positive anomalies relative to rare earth elements with similar partition coefficients during mantle melting. The "high field strength" elements Nb and Ta range from much more depleted than MORB to more enriched. Zr and Hf often exhibit negative anomalies.

While "continental arc" and "oceanic arc" end members provide a useful synopsis of global arc variations, arc compositions vary continuously with the thickness of the crust upon which the arc is built (Fig. 2). Arcs with the same crustal thickness, including "transitional arcs" with Moho depths of ~30 km have similar parental magma abundances (Fig. 2) apart from elements that exhibit large shifts in sediment compositions, such as Ba. Crustal thickness can also change substantially within a single arc, such as the Chilean Southern Volcanic Zone and Central America. In these cases, the variations within the arc track the global variations in arc averages (Turner et al., 2016; Eiler et al., 2005; Turner and Langmuir, 2022a). In Chile's Southern Volcanic Zone, variations in crustal thickness with constant slab thermal parameter show that elemental abundances are not controlled primarily by slab temperature (Fig. 2, Turner et al., 2016).

The greatest compositional variations are seen on the left side of the spider diagram, while the fields overlap on the right side (Fig. 1). There are strong correlations among all incompatible elements that are near to each other on the spider diagram (Kelemen et al., 2003; Turner and Langmuir, 2015a, 2022a), regardless of their classically assumed geochemical affinity (i.e., fluid mobile, sediment-derived, high-field strength, large ion lithophile). The slopes of the REE are steeper in thick-crusted arcs than thin-crusted arcs at all points to the left of Yb, as exhibited by trends in Dy/Yb and La/Sm (Fig. 2d-e). A critical observation is that while the HREE concentrations of all arc averages are lower than MORB, the Dy/Yb ratios of the thick arc segments are all higher than typical MORB (MORB Dy/Yb $<$ 1.7; Gale et al., 2013), which requires that residual garnet be part of the framework for continental arcs built on thick crust.

Turner and Langmuir (2022a) present several lines of evidence that the compositions shown in Fig. 1 are representative of the overall global diversity of arc-front stratovolcano parental magmas, and that differentiation and crustal contamination cannot produce this first-order diversity (see also Turner and Langmuir, 2015a). Crustal processes have long been called upon to account for the global diversity of arcs (Hildreth and Moorbath, 1988; Farner and Lee, 2017), and there is intuitive appeal to the idea that greater crustal thickness simply leads to more extensive magma differentiation and contamination with continental crust. Indeed, the prevalence of differentiated compositions increases with crustal thickness (Farner and Lee, 2017). Simple arguments, however, show that the large and correlated compositional variations (see Figs. 1–2 and Turner and Langmuir, 2022a), cannot be the result of crustal processes and contamination.

The effects of differentiation can be observed empirically by plotting element abundances and ratios vs. Mg# (Fig. 3, Turner and Langmuir, 2015a, 2022a). Because the compositional offsets persist from Mg# of 0.55 to 0.7, it is implausible that they were generated in the crust. This includes the large variations in moderately incompatible elements, such as Nd, highly incompatible elements, such as Th, and elemental ratios such as La/Sm and Dy/Yb (Fig. 3). Because the systematic offsets between different arc segments persist from Mg# 0.55-0.7, we refer to this data collectively as "high Mg#".

The only intra-crustal process that is hypothetically capable of producing this diversity is cryptic contamination that occurs at high Mg# (~0.7) followed by differentiation that lowers Mg# without significantly modifying key abundances and ratios. Some granites are enriched in certain highly incompatible elements, so a contamination model is superficially reasonable, because small amounts of contamination could have large compositional effects. Several lines of evidence, however, show that this is not a viable model. First, Th and Rb abundances in arcs correlate with the flux from subducting sediments, not overlying crust (Plank and Langmuir, 1993). Second, the contaminant would have to be enriched in elements such as Zr, Sr, P, and Ti, but these elements are not usually incompatible during crustal melting or late-stage differentiation due to retention in accessory phases or plagioclase. Third, mixing needs to be consistent for all elements. Some Himalayan granites, for example, have abundances of Sr, Zr, and Ti

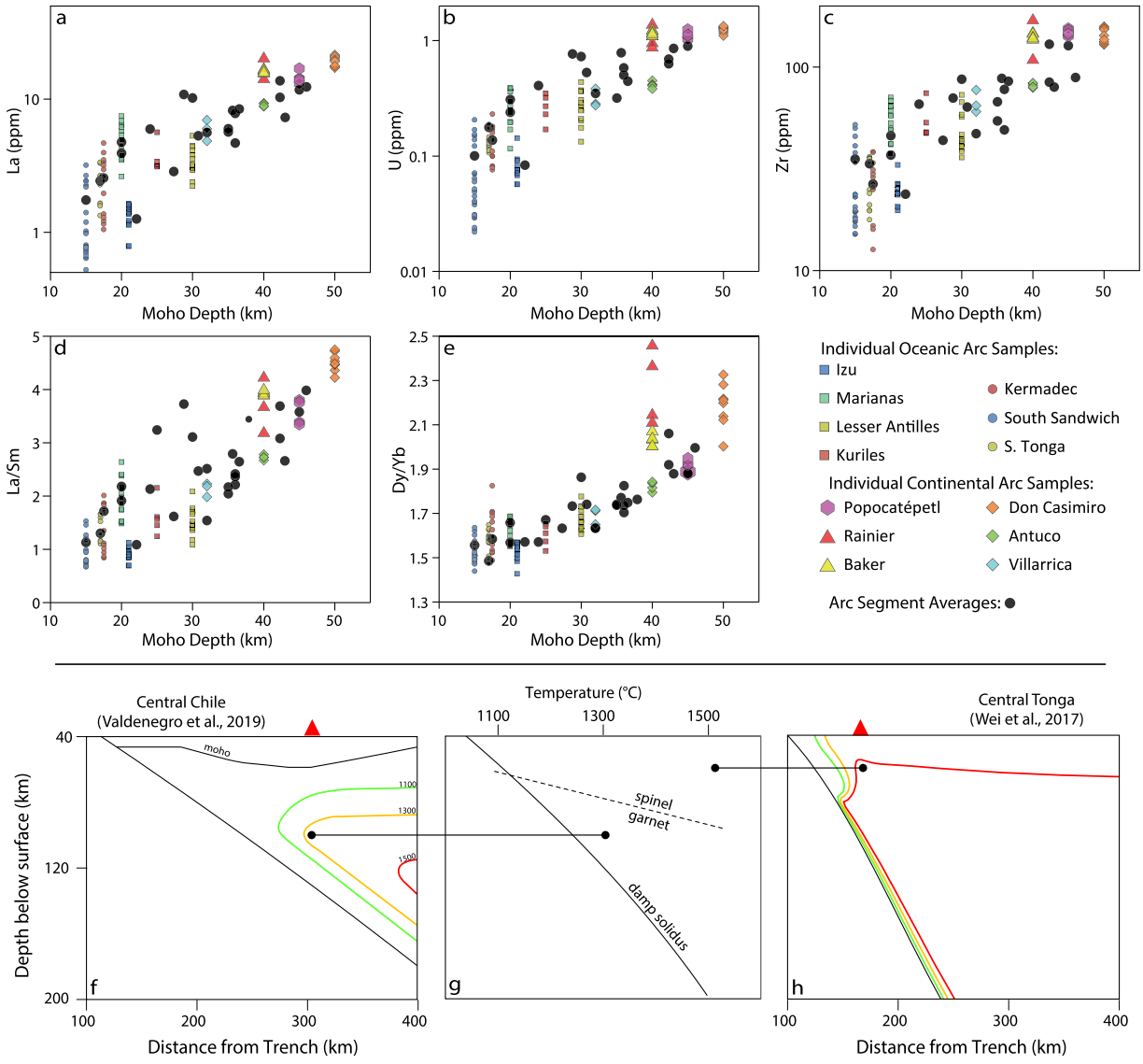

Fig. 2. Panels (a)-(e) show regular relationships between trace element abundances and ratios with the crustal thickness upon which the arc is built. Arc average "6-values" (Turner and Langmuir, 2015a) and data from individual high-Mg# samples (Turner and Langmuir, 2022a) follow the same trends with Moho Depth beneath the arc. High-Mg# samples from the Chilean volcanoes Villarrica, Antuco, and Don Casimiro, which overlie crust with thicknesses of ~30, ~40, and ~50 km, demonstrate that the relationships between crustal thickness and magma chemistry are also observed within individual arc segments that exhibit regular variation in crustal thickness along strike. Panels (f) and (h) depict thermal modeling results for a compressional arc with thick overriding crust and lithosphere (Central Chile, Valdenegro et al., 2019) and an extensional oceanic arc with thin overriding crust and lithosphere (Tonga, Wei et al., 2017). Panel (g) is a phase diagram depicting the 'damp' peridotite solidus (200 °C below the anhydrous solidus of Katz et al., 2003). The spinel-garnet boundary is based on the garnet-in pressures at 1200 °C and 1400 °C in the LC experimental series (which has Cr# = 9.5, similar to the 'DMM' of Workman and Hart, 2005) of Nickel (1986) assuming $\rho = 3$ g/cm^3. The Tonga wedge thermal regime is far hotter relative to the damp solidus, leading to much higher extents of melting. The Chile model predicts lower extents of melting in the garnet stability field. The thermal models suggest that the global geochemical trends with Moho depth in panels (a)-(e) arise in part due to changing extents of melting and residual mineralogy.

(Crawford and Windley, 1990) that fall close to the upper end of the global arc array. If the Himalayan granite were to serve as an assimilant, nearly 100% contamination would be required (producing a rhyolite), though these same rocks have such high Rb and Th abundances that only ~10% contamination is permissible. The low phosphorus contents of these rocks also rule them out as a mixing end member. Finally, a viable contaminant would need to be ubiquitous in arcs with Moho depths > 30 km (Fig. 2), yet neither Turner and Langmuir (2015a) nor Wieser et al. (2019) were able to identify a single silicic rock in the entire GEOROC database with an appropriate composition. To our knowledge, no study has demonstrated a viable quantitative model that can account for the global, systematic behavior that is apparent across the full spectrum of incompatible element abundances of high-Mg# convergent margin magmas via any combination of differentiation and crustal contamination. Instead, we will show that this diversity is quantitatively consistent with mantle processes.

3. Successful and unsuccessful models of arc volcanism

Turner and Langmuir (2022b) reviewed slab dehydration and melting experiments in the context of these global systematics, and found that (1) in agreement with previous studies, the Sr budget of volcanic arcs must be dominated by a component from the altered basaltic ocean crust (AOC) and (2) the excess Sr of arc volcanoes cannot be delivered by a fluid, because numerous experimental fluid partitioning studies show that the solubility of Sr in fluids is too low at the appropriate ranges of pressure, temperature, and bulk composition (see Turner and Langmuir, 2022b, for a detailed discussion). Fluids would be unable to transport the

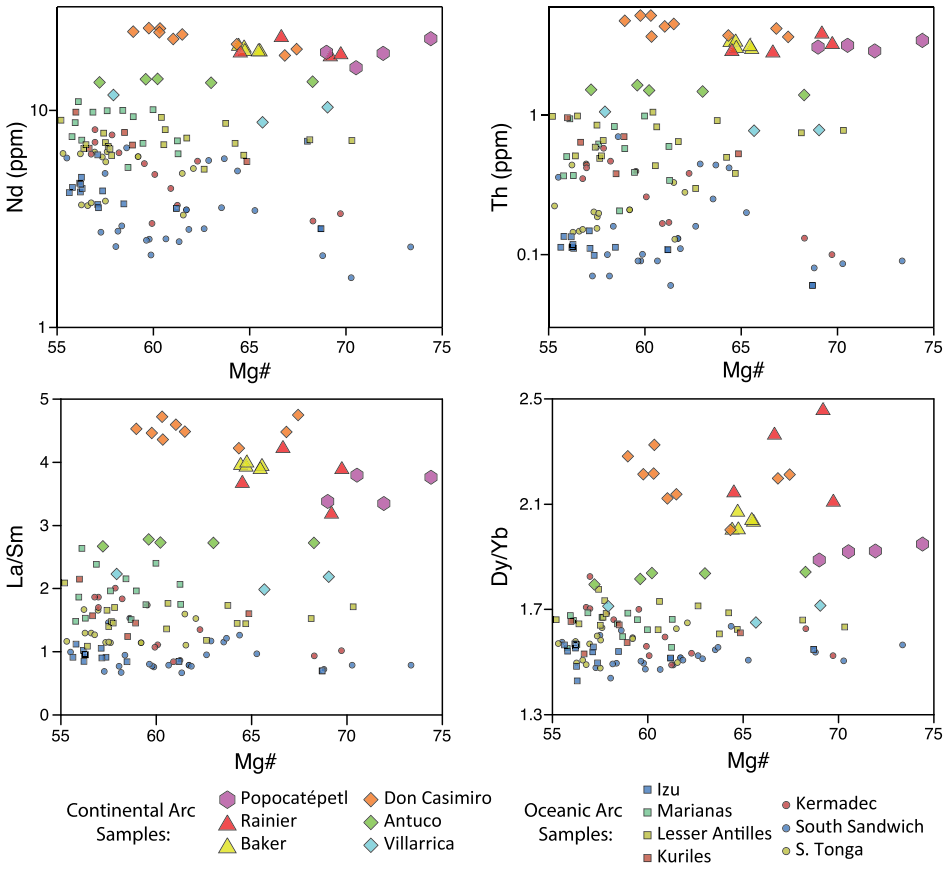

Fig. 3. Plots of element abundances and ratios for individual samples from arc-front stratovolcanoes. Mg# is calculated as molar 100*Mg/(Mg + Fe^{2+}), assuming Fe^{2+} = 0.8*Fe_{total}. Chemical differences among arcs and volcanoes are preserved across the entire range of Mg#, indicating a limited role for differentiation and assimilation (data compilation from Turner and Langmuir, 2022a).

amount of Sr required by mass balance, and the H_2O/Sr ratios of these aqueous fluids would be too high to reproduce the compositions required of arc lava mantle sources. In contrast, experimental melts of natural ocean crust (e.g., Carter et al., 2015; Sisson and Kelemen, 2018) easily meet mass-balance requirements. The melting experiments can also account for the positive Sr anomaly if the slab is moderately oxidized and retains residual epidote (Carter et al., 2015). Using the magnitudes of trace element anomalies as a guide, Turner and Langmuir (2022b) provide models of trace element distribution during AOC and sediment melting that are most consistent with both experiments and arc data.

While the Sr mass-balance arguments require melting of the ocean crust, Turner and Langmuir (2022a) show that varying the amount of slab melt does not control the large global variations in arc element abundances, in contrast to suggestions by Kelemen et al. (2003) and Schmidt and Jagoutz (2017). This model is unsuccessful because even elements such as Zr, Dy and Nb exhibit large global variations (see Fig. 1, Fig. 2c), though these elements do not partition preferentially into slab melts unless temperatures are far higher than the predictions of thermo-mechanical models (e.g., van Keken et al., 2018). Even if the required conditions for Dy mobilization were plausible, the accessory phases capable of retaining the LREE would become exhausted at such high temperatures, resulting in melts with excessive LREE enrichment that lack a positive Sr anomaly. Similar lines of reasoning negate models of slab diapirism, in which the sediment or AOC ascend *en masse* from the slab surface (Turner and Langmuir, 2022a).

There is strong geochemical support, on the other hand, for global control of arc incompatible elemental abundances by variations in the extent of melting in conjunction with variations in ambient mantle enrichment. Moderately incompatible element abundances such as Zr are not heavily impacted by ambient mantle variation and are not strongly partitioned into slab melts (Hermann and Rubatto, 2009; Carter et al., 2015), and yet segment-averaged Zr abundances vary by factor of five (Fig. 2c). The enrichment of moderately incompatible element abundances in continental arcs is most consistent with lower extents of melting. Differing melt extents are a natural consequence of variations in the thermal structure of the mantle wedge as a result of differing upper plate structure and convergence rate (Turner et al., 2016). Fig. 2f-h illustrates this point using recent thermo-mechanical models that are constrained by geophysical observations of heat flow and mantle potential temperatures (Valdenegro et al., 2019; Wei et al., 2017). These models show that arcs under compression with a thick overriding lithosphere have mantle isotherms that are displaced to higher pressures and squeezed away from the wedge corner. The mantle P-T conditions beneath arcs with thick overriding plates are thus closer to the water-bearing mantle solidus (Fig. 2g), resulting in lower total melt fractions.

An alternative possibility is that variations in melt extent result from a variable flux from the slab. Stolper and Newman (1994) showed that increased water correlates with increased extents of melting for the Marianas back-arc basin, and subsequent studies confirmed similar relationships in other back-arc spreading centers (Langmuir et al., 2006; Kelley et al., 2006; Bézos et al., 2009). This model has also been applied to arc-front volcanics. Eiler et al. (2005), for example, adopted this approach to model the arc-front volcanics of Central America and Plank (2013) proposed this mechanism as a potential explanation for the limited range of average water contents observed in olivine-hosted melt inclusions world-

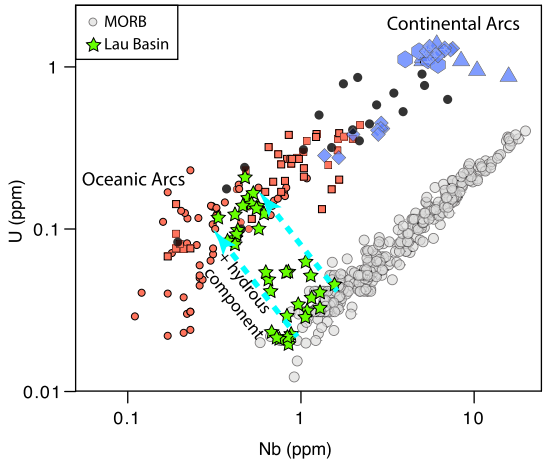

Fig. 4. Arc-front data as in Figs. 2–3 now filled uniformly blue for continental arcs and orange for oceanic arcs. Arc and MORB data each show constant ratios across a large range of concentration. The large range is likely produced by variations in mantle enrichment and extents of melting. The offset reflects the slab contribution to arc data. This is illustrated by back-arc data from the Lau basin that show the combined effect of increasing slab contribution (adding U) and increased extents of melting (lowering Nb) (Bézos et al., 2009). The differing trends between the Lau and arc-front data show that the arc-front trend cannot be produced by variable extents of melting that arise from a varying hydrous slab flux. MORB compilation from Gale et al. (2013). Lau data are from Bézos et al. (2009), Escrig et al. (2012), and Gale et al. (2013). Lau data has been filtered to include only samples with >6 wt% MgO and Zr/Nb between 40 and 65, in order to demonstrate behavior of mafic samples with a depleted ambient mantle composition. (For interpretation of the colors in the figure(s), the reader is referred to the web version of this article.)

wide. In the latter case, it was proposed that higher source water contents would lead to higher extents of melting that buffer the water contents in the resultant magmas.

In back-arc basins, the finding that varying melt extents are controlled by varying source water concentrations is supported by the key observation that the concentrations of elements that do not partition preferentially into slab fluids or hydrous melts ('immobile elements') vary inversely with the concentrations of elements that should be mobilized in hydrous slab liquids ('mobile elements'). There are negative correlations between back-arc basin lava U and Nb abundances, for example, because the slab contributes sufficient U to increase U in the melt despite increasing extents of melting, while Nb simply becomes diluted (Fig. 4). Similar relationships hold for a host of other elements (e.g., K_2O vs. TiO_2). For arc-front stratovolcanoes, however, immobile elements such as Zr, Nb, and Hf correlate positively with mobile elements such as Rb, Sr, Pb, U, and K (Figs. 1-2, 4, Turner and Langmuir, 2015a, 2022a). In addition, melting calculations that include the latent heat of melting and constrain the range of average primary water contents in arcs allow for only about 50% variation in melt extent, rather than the 400% variation indicated by moderately incompatible element abundances (see online supplement). Changes in extent of melting from variable water flux are thus a second order effect, and not the cause of the global systematics addressed here.

While variations in melt extent driven by wedge thermal structure are significant and probably inevitable, they cannot produce the 100x variations in Nb/Yb ratios observed at arcs (Fig. 5a). These two elements are particularly significant because neither are transported efficiently from the slab, thus ambient mantle enrichment and differing melt fractions are the most plausible controls. The range of Nb/Yb in arcs is similar to MORB, where mantle heterogeneity is known to play a major role (Schilling et al., 1983; Langmuir et al., 1992; White, 2015). The offset of arc data to higher Th/Yb is clearly the result of the slab input (as for U abundances, on Fig. 4). The subparallel arrays on the Th/Yb vs Nb/Yb diagram led Pearce (1983) to the conclude that arc and MORB data are best explained by fairly uniform additions of a high-Th/Nb slab component to a mantle that initially has highly variable incompatible element abundances but constant Th/Nb, as found in MORB. An important corollary of this observation is that a significant part of the variation in Th/Yb is also inherited from a heterogenous ambient mantle.

High-Mg# arc magmas also have a large range in isotopic compositions that reflect the combined effects of added slab material and heterogeneity of the ambient mantle. Fig. 5b shows data from arcs, rear-arc monogenetic cones and back-arc spreading centers, MORB (free from plume influences), and ocean island basalts (OIB, specifically PREMA-EM1 OIB). The rear-arc data have been filtered to remove samples that have traces of the subduction signature (see figure caption and Turner and Langmuir, 2022a), thus reflect the large range of ambient mantle compositions flowing towards the arcs. The array of ambient mantle compositions on Fig. 5b overlaps the MORB and OIB data, while the arc data forms a parallel array to the ambient mantle range. Variations in $^{87}Sr/^{86}Sr$ on Fig. 5b are thus analogous to the U abundances and Th/Yb ratio on Figs. 4 and 5a, because U, Th, and Sr are all substantially mobilized in the slab component, unlike Nb and Hf. Arcs show a roughly constant offset from ambient mantle compositions to higher U, Th/Yb, and $^{87}Sr/^{86}Sr$ at all values of Nb, Nb/Yb, and $^{176}Hf/^{177}Hf$, respectively. As highlighted by Hf isotope studies of continental arcs (Straub et al., 2015; Heydolph et al., 2012; and Jacques et al., 2013) as well as Turner and Langmuir (2022a), the Hf isotope enrichment of the thick continental arcs cannot arise from mixing between slab components and a uniformly depleted ambient mantle, which would produce a much shallower slope. Instead, these arcs appear to require an ambient mantle source that is isotopically enriched prior to the addition of slab melts. Therefore, the trace element and isotope systematics on Figs. 4–5 all point to a variable ambient mantle composition (and extents of mantle melting, for the trace elements), with mostly uniform additions of a slab component.

In summary, geochemical characteristics and global variations in trace element and isotopic compositions of arcs are most consistent with slab melting of both AOC and sediment, with similar proportions of melt added to a variable ambient mantle. Global variations in moderately incompatible trace element abundances also require variability in the extent of mantle melting, and residual garnet is required in arcs with thick overriding plates. These qualitative conclusions provide the basis for our quantitative model.

4. Quantifying the relative effects of the slab, wedge, and ambient mantle

To quantitatively assess the various sources of arc magma diversity, we turn first to MORB systematics. MORB derived from enriched mantle sources are commonly distinguished from depleted MORB by the ratio La/Sm, which is only fractionated by low extents of melting. Fig. 6a compares La/Sm and Sm contents of high-MgO MORB from the Mid-Atlantic Ridge with models of progressive melting from different mantle sources (see online supplement for details of melting calculations). For a given source composition, La/Sm varies by only a small amount above 5% melting, whereas Sm abundances co-vary with melt extent. A plot such as Fig. 6a can thus be used to infer the level of source depletion/enrichment and average extent of melting that produced a given mid-ocean ridge basalt.

The different melting trajectories shown on Fig. 6a correspond to three different mantle source compositions. They were calculated as batch melts using published partition coefficients and residual mineral modes that vary with extent of melting. Melts calculated from Workman and Hart (2005)'s 'EDMM' mantle source

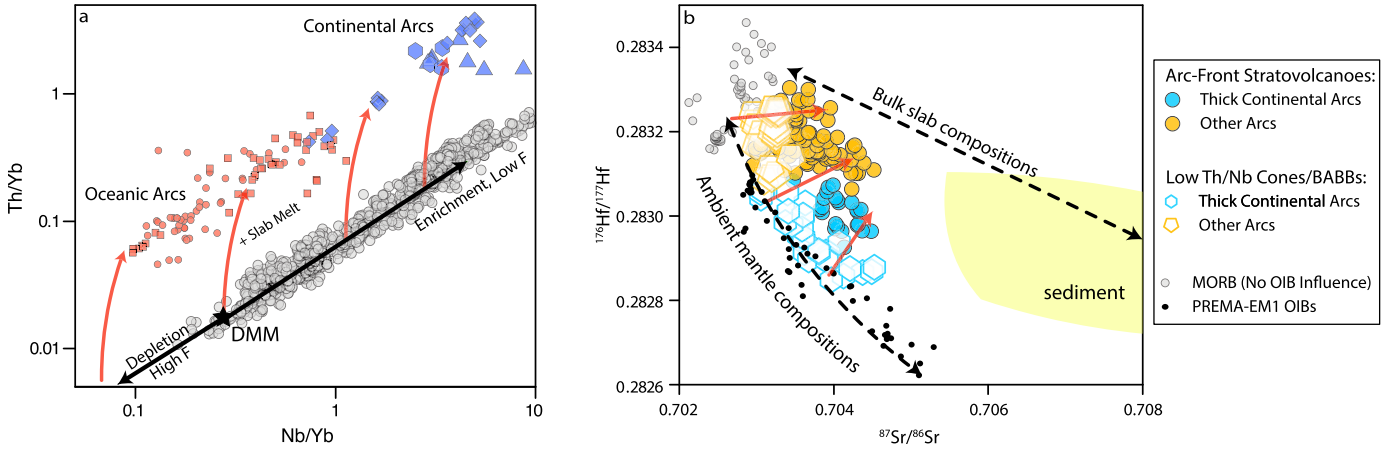

Fig. 5. Trace element and isotope evidence for large ranges in the composition of the ambient mantle beneath global arcs. (a) The "Pearce diagram" shows the 100× range of Nb/Yb. In part, this is due to varying extents of melting but must largely arise from variations in the composition of the ambient mantle. The universal enrichment of Th in arc-front stratovolcano magmas requires sediment melting in all arcs. (b) Hf and Sr isotope variations in arc-front stratovolcanoes, rear-arc samples filtered for a lack of slab influence via Th/Nb < 0.12, EM1 ocean island basalts, and depleted MORB (Hf isotope compilation is available as online supplement). Data from thick crusted continental arcs are blue symbols, all other arcs are orange. Data are omitted when shown to be affected by crustal contamination (e.g., Davidson and Wilson, 2011; Woodhead et al., 2001). Hf isotope variations for ambient mantle, as represented by the rear-arc samples, are parallel to the MORB-EM1 array. Arc samples are parallel the rear-arc samples but offset to higher $^{87}Sr/^{86}Sr$. The diagram is consistent with Hf being less mobile in the slab component and being largely controlled by ambient mantle composition. The slab component significantly increases $^{87}Sr/^{86}Sr$, but by a uniform degree in most arcs. Note that the trace element and isotope figures (panels a and b) are consistent with one another, demonstrating a large range in ambient mantle compositions and a roughly constant slab component.

intersect the middle of the MORB array on the plot of La/Sm vs Sm. The samples are divided into 'Group 1' and 'Group 2' based on whether they fall above or below this model curve. A second 'most depleted' MORB curve has been generated by adjusting the mantle source composition to intersect MORB with the lowest La/Sm (see figure caption). Melting curves are also generated from a source composition inverted from EM1-type OIBs (see online supplement) using an initial mineralogy and reaction coefficients appropriate for higher pressures (to produce melts consistent with the OIBs themselves). The 'EMORB Mantle' melting curve was generated using the EM1-OIB source but with low-pressure mineral modes and reaction coefficients. MORB with La/Sm values above the EM1 and EMORB curves on Fig. 6a are placed into 'Group 3'.

In volcanic arcs, La/Sm is also affected by sediment (Plank, 2005), and probably AOC melt, so the MORB discriminant diagram in Fig. 6a cannot be directly applied to the composition of the mantle wedge. The isotopic composition of the wedge can be determined using rear-arc and monogenetic volcanics that are not greatly impacted by slab material (e.g., Fig. 4 and 5b), though in continental settings these volcanics are often produced by very low extents of melting, significantly fractionating La/Sm (Wieser et al., 2019). The rear-arc volcanics thus provide useful information on the isotopic heterogeneity of the ambient mantle, but not always its trace element composition.

To circumvent these complications, we first consider Nb and Sm, which are less mobile in slab melts (Carter et al., 2015; Hermann and Rubatto, 2009) and thus provide more direct information about the ambient mantle composition and extent of melting for arcs. MORB systematics show that Nb abundances can be used in place of La/Sm as a proxy for source enrichment, because MORB are produced by between 5 and 15% melting (Langmuir et al., 1992), which accounts for most of the variation in Sm, but only 10% of the variation in Nb (Fig. 6b). Furthermore, the melting curve generated using Workman and Hart (2005)'s 'EDMM' mantle source perfectly delineates the 'Group 1' and 'Group 2' MORB on Fig. 6a as well as Fig. 6b, confirming that La/Sm and Nb have similar sensitivities to melt extent and source enrichment. Both La/Sm and Nb thus serve as useful indices of mantle source enrichment, though the Sm vs Nb diagram is more useful in arc settings. As noted by Gale et al. (2011), the most enriched 'Group 3' MORB appear to have been enriched by low degree melts around hot spots. To account for these samples requires a source with higher Nb source abundances than the EM1 OIB source. To match the Nb abundances of the 'Group 3' MORB, the Nb concentration of the 'EMORB Mantle' source has been increased by a factor of two relative to the EM1-OIB source. Since this process is not pertinent to arcs, and given the isotopic affinity between enriched arc data and EM1 (Fig. 5b, Turner et al., 2017; Wieser et al., 2019), we use the unmodified EM1-OIB source for the arc models.

Because slab melts are not entirely devoid of Nb and Sm, the impact of slab components on these elemental abundances must also be considered. Strontium systematics and slab melting experiments indicate ~4-7% slab melts in the mantle sources of arc stratovolcanoes (Turner and Langmuir, 2022b). In the application of the Nb vs. Sm diagram to arc data (Fig. 7), additional melting curves have thus been calculated from each ambient mantle source mixed with 6% of either a "hot" or "cold" slab melt to assess the effects of slab-derived Sm and Nb. Estimates of slab melt compositions are provided in Turner and Langmuir (2022b). This exercise confirms that slab temperature variations would have only a minor impact on this plot.

The arc data cut across the different melting curves on Fig. 7, showing that arcs with enriched ambient mantle sources are generated by lower extents of melting, and arcs with more depleted mantle melt to greater extents (see online supplement for details of melting calculations). As shown by many prior studies, arcs with the lowest incompatible element abundances require mantle sources that are more depleted than even the most depleted MORB mantle (e.g., Woodhead et al., 1993; Schmidt and Jagoutz, 2017). Extra melting curves have thus been generated for a DMM mantle source from which 3% melt has been extracted (black dotted lines, Fig. 7). These curves pass through most of the oceanic arc lava compositions, though some may require sources with even more extensive source depletion. The depletion must be recent because $^{143}Nd/^{144}Nd$ values in these arcs are not elevated relative to MORB (Turner and Langmuir, 2022a). This oft-made observation is consistent with prior melt extraction in back-arc spreading ridges. The continental arc stratovolcanoes, in contrast, require both low extents of mantle melting (5-10%) and more enriched ambient mantle sources. If extents of mantle melting are greater than ~5%, then many of the continental arc volcanics are most consistent

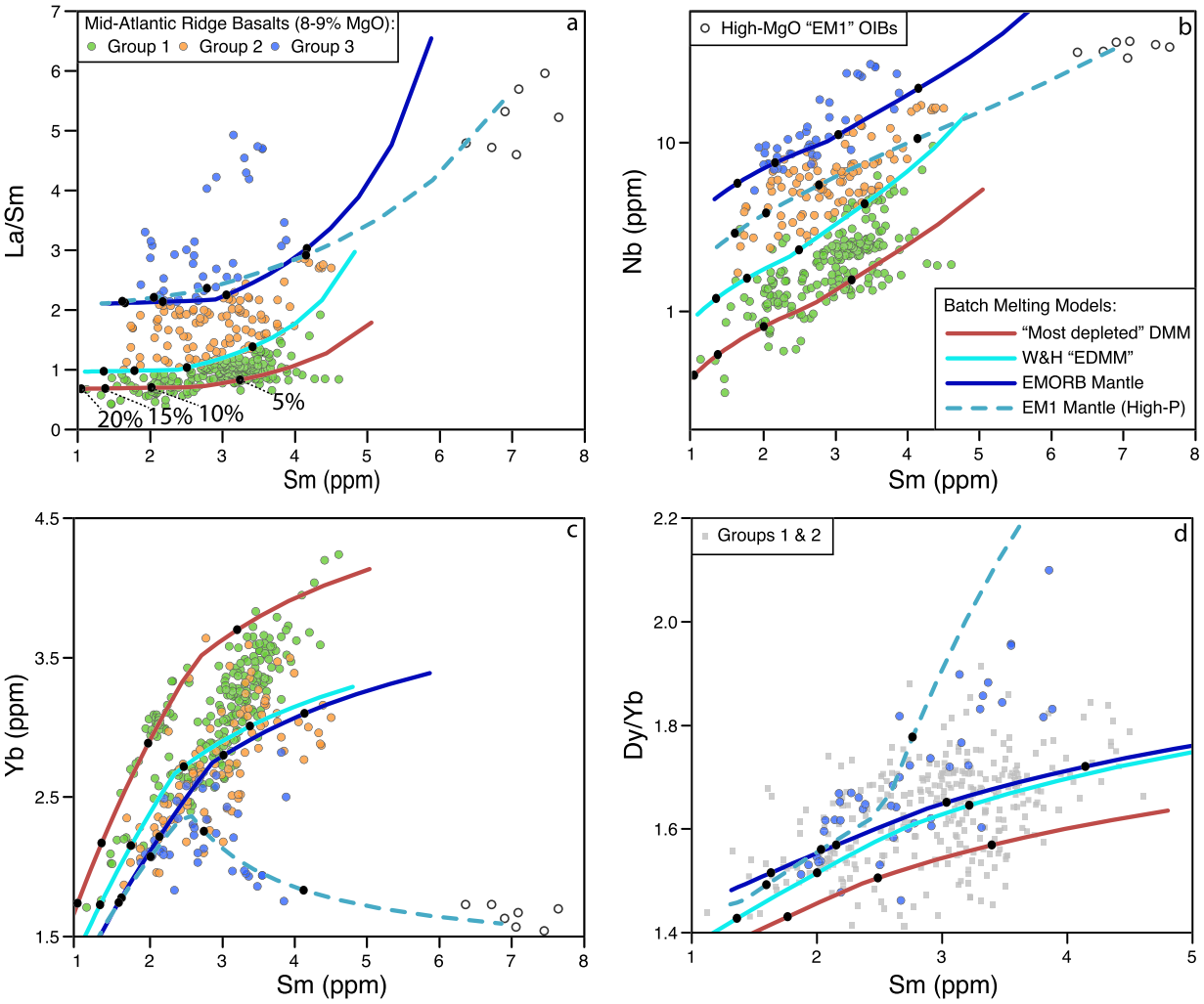

Fig. 6. MORB data from the Mid-Atlantic Ridge with 8-9 wt% MgO (as compiled by Gale et al., 2013) compared to melting models. The MORB are divided into three groups based on La/Sm-Sm. Melting curves for MORB are calculated using pyroxene partition coefficients from Yao et al. (2012), and olivine partition coefficients from Salters and Stracke (2004) at melt extents from 1% to 25% (black dots designate 5% intervals from 5% to 20%). The light blue curve was generated using the "EDMM" mantle source from Workman and Hart (2005). The mantle source composition for the dark blue "most depleted" DMM curve was selected to fit the lower bounds of the MORB data (0.065 ppm Nb, 4.91 ppm Zr, 0.094 ppm La, 0.2415 ppm Sm). The "EM1 Mantle" source composition was calculated by inverting from an averaged composition of enriched EM1-OIB from Pitcairn and Gough (as in Turner et al., 2017 and Wieser et al., 2019), but with minor updates as described in the online supplement. The "High-P" melting trajectory was generated using cpx and garnet partition coefficients consistent with the experiments of Salters et al. (2002) but smoothed based on atomic radii to eliminate noise (see online supplement). Melting of the EM1 source using the low-pressure partition coefficients would generate melts with lower Nb than the Group 3 MORB, therefore an additional 'EMORB' source with the same composition as the EM1 source but 2× more Nb is used to generate the red low-P EMORB source melting curve. Additional details of the melting model are available in the online supplement.

with an EM1-like source, as also inferred from the isotope systematics (Fig. 5b).

Enriched MORB compositions commonly require a source with residual garnet, which implies higher pressures of melt generation (Asimow and Langmuir, 2003). The garnet signature is most apparent from HREE trends, where the most enriched 'Group 3' Atlantic MORB samples fall below the low-pressure melting curve for Sm vs Yb, indicating retention of Yb (Fig. 6c). The ratio Dy/Yb is a sensitive indicator of garnet, and samples with Dy/Yb > ~1.7 require garnet during mantle melting (Fig. 6d).

The strong global correlation between arc crustal thickness and Dy/Yb among both high-Mg# arc-front stratovolcano data and averaged arc segment compositions (Fig. 2e) indicates residual garnet for thick-crusted arcs but not for island arcs. Because Dy is not sufficiently mobilized by slab melts (Turner and Langmuir, 2022a) this signal must arise due to residual garnet in the mantle wedge. Thermal models and experimental data also confirm that residual garnet in the mantle wedge is likely during the generation of continental arc magmas (Fig. 2f-g). While garnet is not stable along the anhydrous solidus until higher pressures than expected in the mantle wedge (Robinson and Wood, 1998; Schmidt and Jagoutz, 2017), under the lower temperature hydrous melting conditions beneath arcs the garnet-in boundary may be even lower than 2 GPa (Gaetani et al., 2003) and garnet can persist to higher extents of melting (Hall, 1999). These constraints are thus consistent with the presence of residual garnet for continental arcs even within the "core" of the mantle wedge, where most melt generation occurs. The fact that arcs built on >35 km thick crust all have Dy/Yb > 1.7 is therefore likely to reflect to residual garnet during melt generation, just as for MORB. While the major element compositions of many arc magmas appear to indicate a shallow final magma equilibration close to the base of the crust, there is no reason that this would substantially affect incompatible trace element ratios nor erase the garnet trace element signature (Till, 2017). Therefore, trace element data, experiments on phase stability, and numerical simulations all support models of continental arc melt generation in the garnet stability field, and the quantitative analysis here will proceed on this basis.

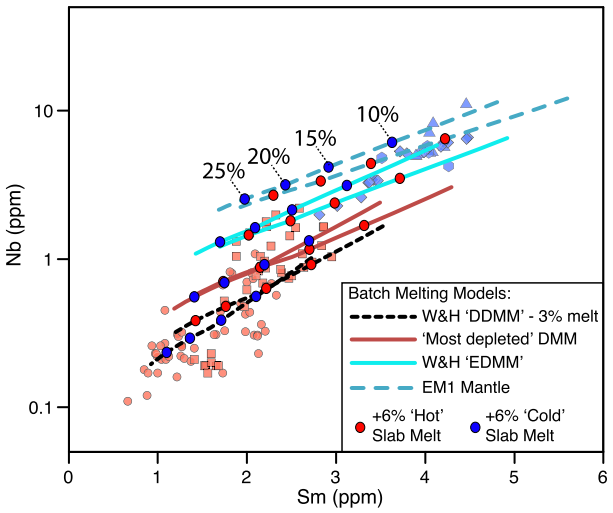

Fig. 7. Global arc data (as in Figs. 1–3) compared to melting curves for four different mantle source compositions. Blue symbols are continental arc data, orange are oceanic arc data, as in Fig. 4. Mantle sources are the same as Fig. 6, but with the addition of an extra-depleted mantle source calculated using the 'DDMM' source of Workman and Hart (2005) after extraction of 3% batch melt using the partition coefficients and mineral modes of Salters and Stracke (2004), though assuming no fractionation occurs between Nd, Zr, and Hf or between elements more incompatible than La. Model slab melts with either 0.5 or 1 ppm Nb, and either 1.5 or 2.6 ppm Sm were added to the mantle sources for the 'Cold' and 'Hot' slab scenarios, respectively. These values are consistent with the AOC melt compositions determined by Turner and Langmuir (2022b), but with Sm abundances adjusted slightly upward to reflect a sediment contribution. The model curves are consistent with the most enriched arc compositions derived by both enriched mantle sources and low extents of melting, while the most depleted arc data require higher extents of melting and a more depleted mantle source than even the dark blue 'most depleted' DMM source (see Fig. 6). See online supplement for additional details of hydrous melting model.

The quantitative predictions of ambient mantle composition for arcs on Fig. 6 range from the Workman and Hart (2005)'s DMM source following 3% melt extraction, for oceanic arcs, to an ambient mantle with EM1-like trace element abundances, for continental arcs. The range of extents of melting are constrained by Nb and Sm abundances with melting beginning in the garnet stability field for enriched continental arcs.

Fig. 8 demonstrates that this modeling approach reproduces the first-order global chemical systematics among arc-front volcanics (as summarized by Turner and Langmuir, 2022a). The mantle sources used for the forward models on Fig. 8 are modified by addition of sediment melt and AOC melt in all cases. The sediment melt composition is calculated using partition coefficients from Turner and Langmuir (2022b), and assuming F = 0.4, while the AOC melts are the 'cold' and 'hot' AOC melt compositions of Turner and Langmuir (2022b) which assume F = 0.15 and F = 0.3. The slab contributions to the arc mantle source are held constant in all cases, with 0.5% sediment melt and 6% AOC melt.

The covariation between Nd and Dy/Yb arises primarily from variations in extents of mantle wedge melting, which are compounded by decreasing proportions of residual garnet at higher F in continental arcs (Fig. 8a). The contrast between melting of garnet and spinel peridotite produces the orthogonal arrays of data on Fig. 8b, showing that Nd and Yb are positively correlated among island arc lavas with no garnet signature, but negatively correlated among continental arcs where garnet is residual during melting. For the continental arc array, the potential effects of hotter slab temperatures are also illustrated, though such effects are minor for Sm, Nd, Dy, and Yb.

Global variations in Sr/Nd are strongly influenced by ambient mantle heterogeneity (Fig. 8c) because the slab component has a greater influence on more depleted mantle. The Sr/Nd relationships also indicate a role for variations in slab temperature. Hot slab melts should have lower Sr/Nd due to both larger extents of slab melting and decreasing stability of REE bearing accessory phases (Turner and Langmuir, 2022b) and seem to be required when Sr/Nd < 40.

The model also accounts well for the global correlation between Sm and La/Sm (Fig. 8d). Most variation in Sm occurs due to varying extents of melting, but the total variation in La/Sm requires ambient wedge heterogeneity. The correlated data require a decrease in extent of melting with increasing ambient mantle enrichment, as inferred from Sm vs Nb (Fig. 7).

While the elements modeled on Fig. 8 are not generally dominated by the sediment component, other arc elemental abundances, particularly Ba and Th, are strongly correlated with the sediment compositions subducting in each trench (Plank and Langmuir, 1993). Despite these correlations, variations in Ba/Th vs La/Sm (Fig. 9) are often interpreted as the result of distinct components from aqueous fluids, which generate high Ba/Th, and slab melts, which generate high La/Sm (e.g., Elliott, 2003, and references therein). If sediment dominates both the Ba and Th budgets, however, an internally consistent interpretation requires instead that high-Ba/Th arc lavas simply reflect high-Ba/Th sediment melts. How could Ba be controlled by the sediment flux and also be fluid-controlled? Furthermore, Ba abundances in AOC are too low to account for the needed Ba contents of arc magmas.

The modeling framework presented here resolves these contradictions by incorporating variable mantle wedge and sediment compositions. The different colored stars on Fig. 9 are produced by variations in wedge composition and extent of melting absent any slab addition. Variations in La/Sm largely arise due to enriched mantle and low extents of melting in continental arcs and depleted mantle and high extents of melting in oceanic arcs. The slab component is not a constant because of very different Ba contents of sediments. From each star, mixing arrays are generated to slab melts (combining AOC and sediment melt) that include high Ba sediments (dashed lines) and low Ba sediments (solid lines). Because the slab melt addition has a greater impact on the highly depleted mantle, the high Ba slab melt leads to the highest Ba/Th only when La/Sm is low. Low Ba/Th is thus associated with high La/Sm because the impact of slab addition is lessened by enriched ambient mantle, and also because these continental arcs are dominated by terrigenous sediment, which has low Ba/Th.

This modeling approach provides a straightforward method to model all commonly measured incompatible trace element abundances. Example models of high-Mg# compositions from oceanic and continental arcs are shown on Fig. 10. Using sediment and ambient mantle compositions specific to each arc, as well as variations in extents of melting, the models produce the full trace element patterns. The large variations in Ba/Th in the two patterns result from the effects of differing sediment and ambient mantle. Other ratios that are less dominated by recycled sediment, such as K/La or Sr/Nd, are more likely to reflect variations in slab temperature. The modeling framework thus successfully and quantitatively reproduces the essential differences that are characteristic of global arc stratovolcano variations.

While the model is successful in reproducing global trends, there are obviously several extensions, exceptions, and further tests that are necessary. For example, the model predicts Cs abundances for Mt. Baker in the High Cascades that are too high (see Fig. 10). This may be because Cs is more soluble in fluids than any of the other plotted elements (Spandler et al., 2007), leading to Cs loss during early sediment dehydration beneath the forearc. Similar findings have been reported for Cs from the modeling of Class et al. (2000) in the Aleutians and Wieser et al. (2019) in Central Chile. There are also exceptional stratovolcanoes such as the highly enriched lavas of Costa Rica and the alkaline samples from Grenada,

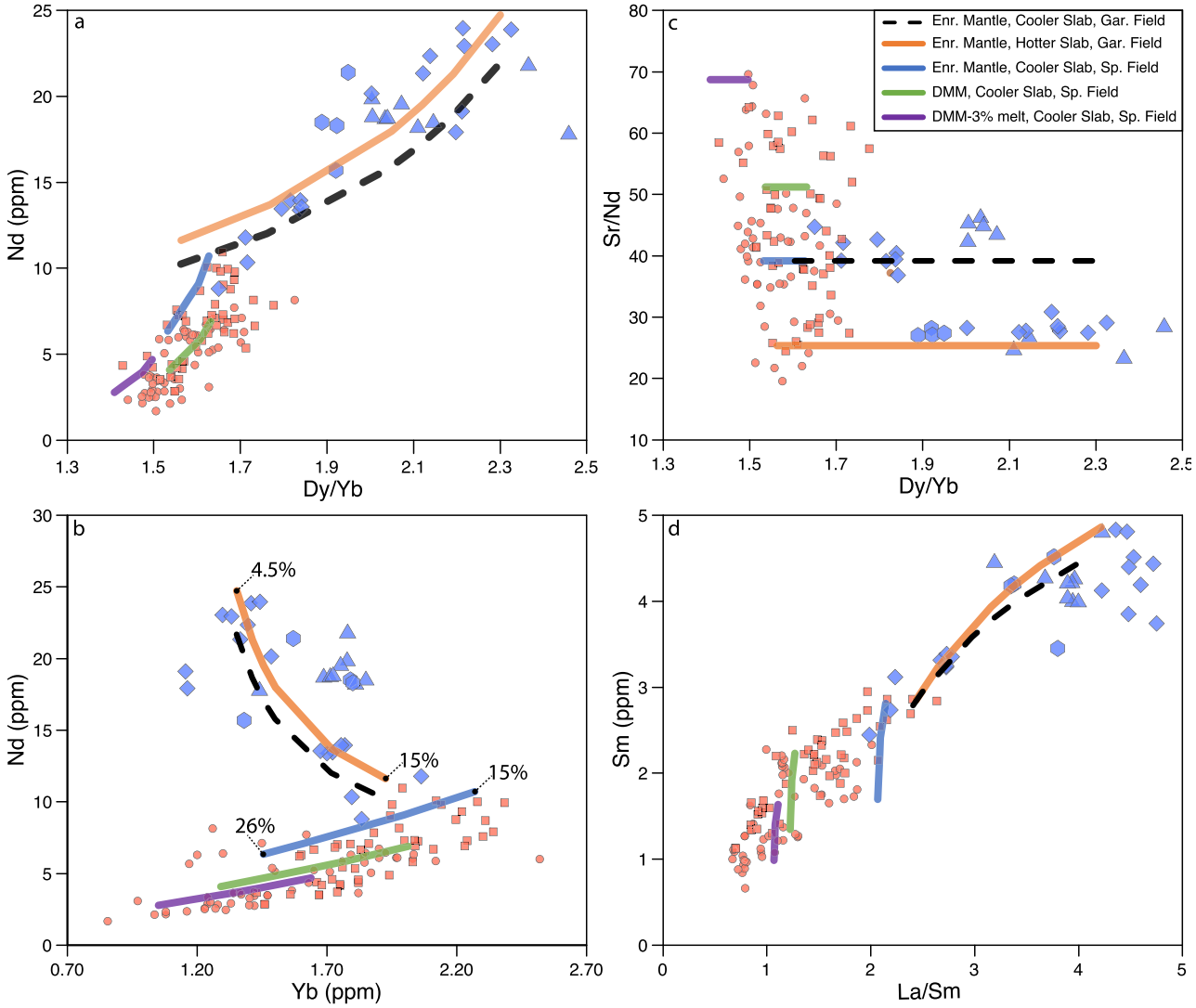

Fig. 8. Comparison of global high-Mg# arc data (as on Figs. 1–5) and model outputs. Each model curve represents a range of melting extents from a single mantle composition. The orange and black curves, which pass through the blue continental arc data, vary from F = .045 to F = .15 with melting beginning in the garnet stability field, while the purple, green, and blue curves pass through the oceanic arc data with F = .15 to F = .26 (see online supplement for details of melting model). With the exception of the orange curve, the mantle composition changes exclusively due to variation in the ambient mantle composition – the same slab melt composition is always added in the same proportions (mixing proportions are 0.5% sediment melt and 5% AOC melt). Slab melts are calculated as in Turner and Langmuir (2022b), using the lowest temperature D values for sediment melting and the 'colder' AOC melt composition. The average bulk composition of core DSDP 1232 (Turner et al., 2017) is used in all cases, though the elemental abundances and ratios on these plots are not very sensitive to the particular sediment used. The orange curve differs from the dashed black curve by incorporating a different slab melt composition, using the 'hotter' AOC melt composition and the maximum temperature D values for sediment melting from Turner and Langmuir (2022b). The range of model parameters were selected based on the constraints described in the text, and in all cases are consistent with the systematic variations observed among the arc data. The model outputs demonstrate that for these elements the large global variations can be produced primarily by changes in the ambient mantle composition and extent of mantle melting. Only Sr/Nd is substantially sensitive to slab temperature, though it is notable that even Sr/Nd is more significantly altered by changes in ambient mantle composition.

arc stratovolcanoes subjected to intra-arc rifting, as well as lavas erupted from minor eruptive centers and monogenetic cones. In all these cases, the proposed framework is likely to provide insights and impetus for directions of future study. The model also needs to be applied to the large regional variations that occur in some arcs, such as Central America (Patino et al., 2000) and the Marianas (Elliott et al., 1997). The success of the model in explaining these regional variations is explored elsewhere (Turner and Langmuir, in preparation).

5. Conclusions

Arc magmas exhibit large ranges in trace element abundances and isotopic ratios. To account for these variations, many have called upon a relatively uniform and depleted mantle wedge that is modified by variable slab components controlled by the temperature of the subducting slab. This model fails the natural experiment of southern Chile where half the global range in arc geochemistry is observed with no change in slab temperature (Turner et al., 2016). A predominant role for melting variations in response to variable water addition from the slab is also untenable for explaining the global variations. Variations in extent of melting caused by changes in wedge thermal structure account for much of the variability of global arc data, but cannot account for the isotopic variations, nor the extreme variations in many incompatible element abundances that exist among high-Mg# samples.

A successful model that accounts for global variations must include ambient mantle compositions that range from more depleted than ocean ridge basalts to as enriched as some ocean island basalts. Ambient mantle wedge variation is the dominant

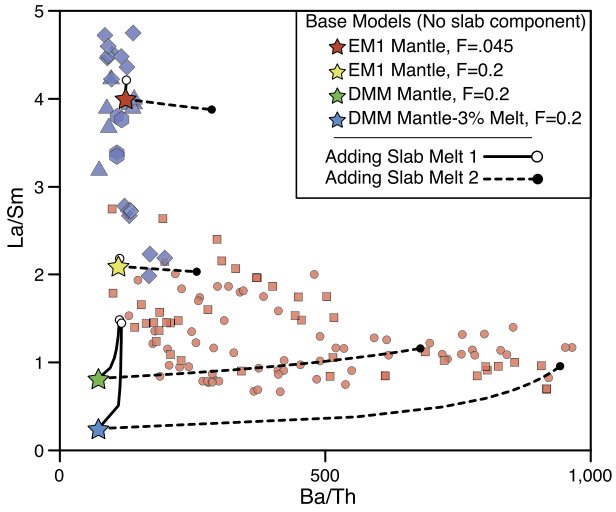

Fig. 9. A demonstration of how variations in sediment composition, ambient mantle enrichment, and extent of mantle melting can reproduce the hyperbolic trend in La/Sm vs Ba/Th that is often attributed to varying control of sediment melts vs aqueous fluids. The different colored stars are generated by melting different ambient mantle compositions (as in Figs. 6–8) absent the addition of a slab component. The curves extending from those stars demonstrate the effects of adding either a terrigenous sediment (DSDP 1232 of Turner et al., 2017) or a high Ba sediment (the lower section of ODP 495 of Patino et al., 2000). 'Slab Melt 1' mixes to a maximum of 6% 'hotter' AOC melt and .7% sediment melt using the high T sediment melting D values of Turner and Langmuir (2022b), while 'Slab Melt 2' mixes to a maximum of 6% 'colder' AOC melt and 0.2% low T sediment melt. Note that the slab component has much larger influence as the mantle becomes depleted, which causes arcs with depleted ambient to end up with much higher Ba/Th. The combination of varying mantle wedge and sediment compositions leads to the hyperbolic array of arc data without an aqueous fluid component. Because both Ba and Th are dominantly controlled by subducted sediment (Plank and Langmuir, 1993), the Ba/Th ratio must also be controlled largely by the sediment composition, and potentially the residual phases present during slab melting.

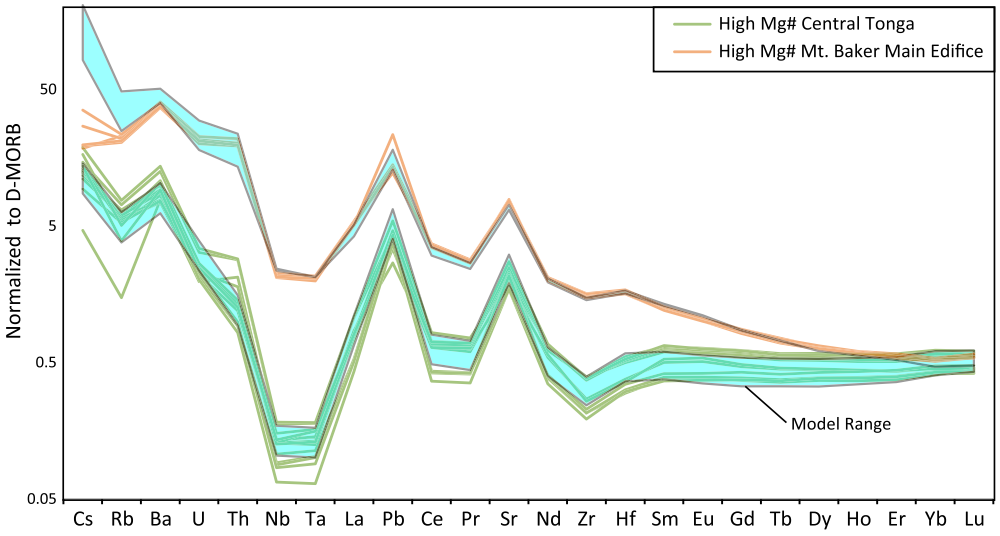

Fig. 10. A comparison of model outputs to the compositions of high-Mg# samples from Central Tonga and Mt. Baker, representing island and continental arc, respectively. The Tongan model incorporates the 'colder' AOC melt (5% of source) and a sediment melt (0.2% of source) calculated assuming 40% sediment melting and D's close to the 'cold' end-member in Turner and Langmuir (2022b), mixed into an ambient mantle starting from Workman and Hart (2005)'s DMM composition followed by an additional 5% melt extraction. The range of model outputs correspond to extents of mantle melting between 15 and 30% followed by 30% olivine fractionation. The Mt. Baker model uses an ambient mantle produced by mixing 70% DMM and 30% EM1 mantle (see online supplement), 7% 'moderate' AOC melt, and between 1% and 1.7% sediment melt calculated using either the average or 'hot' sediment melting Ds of Turner and Langmuir (2022b) and either the bulk Cascades sediment provided by Plank (2013) or the site 888 bulk average of Mullen et al. (2017). Mantle melting extents are 7% for the Mt. Baker model followed by 20% olivine fractionation. The models produce good fits to the data except for Cs for Mt. Baker, which may have been lost from the sediment during early dehydration in the forearc.

control on global variations in Hf and Nd isotope ratios as well as ratios of some incompatible elements. Having ambient mantle vary similarly to what is observed at ocean ridges is both sensible and consistent with the diverse tectonic environments feeding the mantle wedge by corner flow.

A slab component consisting of ocean crust and sediment melts (Turner and Langmuir, 2022b) mixes into the variable ambient mantle wedge. The more depleted the wedge, the more prominent the influence of the slab component. The modified mantle wedge is melted to varying extents, with the pressure and extent of melting controlled by the wedge thermal structure that is in turn largely controlled by the thickness of the overlying lithosphere. Oceanic arcs have thin lithosphere and often have back-arc spreading which depletes the ambient mantle. As a result, depleted mantle and large extents of melting coincide, giving rise to very low incompatible element abundances. Continental arcs have thick lithosphere and are adjacent to sub-continental lithosphere which is often enriched by metasomatism, leading to enriched mantle and low extents of melting. Many arcs, such as the Central and Eastern Aleutians, show intermediate behavior. Variations in man-

tle composition and extents of melting are so predominant that variations in elemental mobility caused by differing slab temperatures become second-order effects.

Continental arcs have low Yb abundances and high Dy/Yb ratios. A comparison to MORB data shows that the high Dy/Yb requires garnet in the residue, which is also consistent with experimental constraints on garnet stability during hydrous melting.

Using inferences from MORB to constrain melting effects, Nd and Hf isotope data to constrain ambient mantle source, and experimental data on melting of sediment and altered ocean crust, it is possible to construct a quantitative model that reproduces global arc data. This modeling framework accounts for both specific compositions and global systematics of the geochemistry of arc stratovolcanoes, a standard that competing models should also be required to meet. The essential ingredients of the model are that AOC melts in all arcs, that variations in composition of the mantle wedge are essential, that extents of melting vary in response to wedge thermal structure, and that garnet is a residual phase during initial melting of many continental arcs. For more detailed modeling of individual arcs, the specific sedimentary compositions and their variability and fluxes become important. The framework provided here provides a baseline upon which such variations can be more carefully evaluated.

CRediT authorship contribution statement

S. Turner's contributions to this work included: Conceptualization, Data curation, Quantitative analysis and modeling, Visualization, and Writing. **C. Langmuir's** contributions to this work included: Conceptualization and Writing.

Declaration of competing interest

The authors declare that they have no known competing financial interests or personal relationships that could have appeared to influence the work reported in this paper.

Acknowledgements

The authors thank Tom Sisson and one anonymous reviewer for constructive comments which substantially improved this manuscript. This work was supported by NSF grant EAR-1939080 to the University of Massachusetts Amherst and NSF grants OCE-1634421 and EAR-0948511 to Harvard University.

Appendix A. Supplementary material

Supplementary material related to this article can be found online at https://doi.org/10.1016/j.epsl.2022.117411.

References

Asimow, P.D., Langmuir, C.H., 2003. The importance of water to oceanic mantle melting regimes. Nature 421, 815–820.
Bezard, R., Davidson, J.P., Turner, S., Macpherson, C.G., Lindsay, J.M., Boyce, A.J., 2014. Assimilation of sediments embedded in the oceanic arc crust: myth or reality? Earth Planet. Sci. Lett. 395, 51–60.
Bézos, A., Escrig, S., Langmuir, C.H., Michael, P.J., Asimow, P.D., 2009. Origins of chemical diversity of back-arc basin basalts: a segment-scale study of the Eastern Lau Spreading Center. J. Geophys. Res., Solid Earth 114.
Carr, M., Feigenson, M., Bennett, E., 1990. Incompatible element and isotopic evidence for tectonic control of source mixing and melt extraction along the Central American arc. Contrib. Mineral. Petrol. 105, 369–380.
Carter, L.B., Skora, S., Blundy, J., De Hoog, J., Elliott, T., 2015. An experimental study of trace element fluxes from subducted oceanic crust. J. Petrol. 56, 1585–1606.
Class, C., Miller, D.M., Goldstein, S.L., Langmuir, C.H., 2000. Distinguishing melt and fluid subduction components in Umnak Volcanics, Aleutian Arc. Geochem. Geophys. Geosyst. 1.
Conrey, R.M., Sherrod, D.R., Hooper, P.R., Swanson, D.A., 1997. Diverse primitive magmas in the Cascade arc, northern Oregon and southern Washington. Can. Mineral. 35, 367–396.
Crawford, M.B., Windley, B.F., 1990. Leucogranites of the Himalaya/Karakoram: implications for magmatic evolution within collisional belts and the study of collision-related leucogranite petrogenesis. J. Volcanol. Geotherm. Res. 44, 1–19.
Davidson, J., Wilson, M., 2011. Differentiation and source processes at Mt Pelee and the Quill; active volcanoes in the Lesser Antilles arc. J. Petrol. 52, 1493–1531.
Davidson, J.P., Harmon, R.S., 1989. Oxygen isotope constraints on the petrogenesis of volcanic arc magmas from Martinique, Lesser Antilles. Earth Planet. Sci. Lett. 95, 255–270.
Dungan, M.A., Wulff, A., Thompson, R., 2001. Eruptive stratigraphy of the Tatara–San Pedro complex, 36 S, Southern Volcanic Zone, Chilean Andes: reconstruction method and implications for magma evolution at long-lived arc volcanic centers. J. Petrol. 42, 555–626.
Eiler, J.M., Carr, M.J., Reagan, M., Stolper, E., 2005. Oxygen isotope constraints on the sources of Central American arc lavas. Geochem. Geophys. Geosyst. 6.
Ellam, R., Hawkesworth, C., 1988. Elemental and isotopic variations in subduction related basalts: evidence for a three component model. Contrib. Mineral. Petrol. 98, 72–80.
Elliott, T., 2003. Tracers of the Slab. Geophysical Monograph, vol. 138. American Geophysical Union, pp. 23–46.
Elliott, T., Plank, T., Zindler, A., White, W., Bourdon, B., 1997. Element transport from slab to volcanic front at the Mariana arc. J. Geophys. Res., Solid Earth 1978–2012 (102), 14991–15019.
Escrig, S., Bézos, A., Langmuir, C., Michael, P., Arculus, R., 2012. Characterizing the effect of mantle source, subduction input and melting in the Fonualei Spreading Center, Lau Basin: constraints on the origin of the boninitic signature of the back-arc lavas. Geochem. Geophys. Geosyst. 13.
Farner, M.J., Lee, C.-T.A., 2017. Effects of crustal thickness on magmatic differentiation in subduction zone volcanism: a global study. Earth Planet. Sci. Lett. 470, 96–107.
Freymuth, H., Ivko, B., Gill, J.B., Tamura, Y., Elliott, T., 2016. Thorium isotope evidence for melting of the mafic oceanic crust beneath the Izu arc. Geochim. Cosmochim. Acta 186, 49–70.
Gaetani, G.A., Kent, A.J., Grove, T.L., Hutcheon, I.D., Stolper, E.M., 2003. Mineral/melt partitioning of trace elements during hydrous peridotite partial melting. Contrib. Mineral. Petrol. 145, 391–405.
Gale, A., Dalton, C.A., Langmuir, C.H., Su, Y., Schilling, J.G., 2013. The mean composition of ocean ridge basalts. Geochem. Geophys. Geosyst. 14, 489–518.
Gale, A., Escrig, S., Gier, E.J., Langmuir, C.H., Goldstein, S.L., 2011. Enriched basalts at segment centers: The Lucky Strike (37 17′ N) and Menez Gwen (37 50′ N) segments of the Mid-Atlantic Ridge. Geochem. Geophys. Geosyst. 12.
Gazel, E., Hayes, J.L., Hoernle, K., Kelemen, P., Everson, E., Holbrook, W.S., Hauff, F., van den Bogaard, P., Vance, E.A., Chu, S., 2015. Continental crust generated in oceanic arcs. Nat. Geosci. 8, 321–327.
Gill, J.B., 1981. Orogenic Andesites and Plate Tectonics. Springer, pp. 1–12.
Hall, L., 1999. The Effect of Water on Mantle Melting. University of Bristol.
Handley, H.K., Blichert-Toft, J., Gertisser, R., Macpherson, C.G., Turner, S.P., Zaennudin, A., Abdurrachman, M., 2014. Insights from Pb and O isotopes into along-arc variations in subduction inputs and crustal assimilation for volcanic rocks in Java, Sunda arc, Indonesia. Geochim. Cosmochim. Acta 139, 205–226.
Hermann, J., Rubatto, D., 2009. Accessory phase control on the trace element signature of sediment melts in subduction zones. Chem. Geol. 265, 512–526.
Heydolph, K., Hoernle, K., Hauff, F., van den Bogaard, P., Portnyagin, M., Bindeman, I., Garbe-Schönberg, D., 2012. Along and across arc geochemical variations in NW Central America: evidence for involvement of lithospheric pyroxenite. Geochim. Cosmochim. Acta 84, 459–491.
Hildreth, W., Moorbath, S., 1988. Crustal contributions to arc magmatism in the Andes of central Chile. Contrib. Mineral. Petrol. 98, 455–489.
Jacques, G., Hoernle, K., Gill, J., Hauff, F., Wehrmann, H., Garbe-Schönberg, D., van den Bogaard, P., Bindeman, I., Lara, L., 2013. Across-arc geochemical variations in the Southern Volcanic Zone, Chile (34.5–38.0 S): constraints on mantle wedge and slab input compositions. Geochim. Cosmochim. Acta 123, 218–243.
Johnson, M.C., Plank, T., 2000. Dehydration and melting experiments constrain the fate of subducted sediments. Geochem. Geophys. Geosyst. 1.
Katz, R.F., Spiegelman, M., Langmuir, C.H., 2003. A new parameterization of hydrous mantle melting. Geochem. Geophys. Geosyst. 4.
Kay, R.W., 1980. Volcanic arc magmas: implications of a melting-mixing model for element recycling in the crust-upper mantle system. J. Geol., 497–522.
Kelemen, P.B., Hanghøj, K., Greene, A., 2003. One view of the geochemistry of subduction-related magmatic arcs, with an emphasis on primitive andesite and lower crust. In: Treatise on Geochemistry, vol. 3, p. 659.
Kelley, K.A., Plank, T., Grove, T.L., Stolper, E.M., Newman, S., Hauri, E., 2006. Mantle melting as a function of water content beneath back-arc basins. J. Geophys. Res., Solid Earth 111.
Kimura, J.-I., 2017. Modeling chemical geodynamics of subduction zones using the Arc Basalt Simulator version 5. Geosphere 13, 992–1025.
Klimm, K., Blundy, J.D., Green, T.H., 2008. Trace element partitioning and accessory phase saturation during H2O-saturated melting of basalt with implications for subduction zone chemical fluxes. J. Petrol. 49, 523–553.

Langmuir, C., Bezos, A., Escrig, S., Parman, S., 2006. Chemical systematics and hydrous melting of the mantle in back-arc basins. In: Back-Arc Spreading Systems: Geological, Biological, Chemical, and Physical Interactions, pp. 87–146.
Langmuir, C.H., Klein, E.M., Plank, T., 1992. Petrological systematics of mid-ocean ridge basalts: constraints on melt generation beneath ocean ridges. In: Mantle Flow and Melt Generation at Mid-Ocean Ridges, vol. 71, pp. 183–280.
Marschall, H.R., Schumacher, J.C., 2012. Arc magmas sourced from mélange diapirs in subduction zones. Nat. Geosci. 5, 862–867.
Martin, E., Bindeman, I., Grove, T., 2011. The origin of high-Mg magmas in Mt Shasta and Medicine Lake volcanoes, Cascade Arc (California): higher and lower than mantle oxygen isotope signatures attributed to current and past subduction. Contrib. Mineral. Petrol. 162, 945.
Miller, D.M., Langmuir, C.H., Goldstein, S.L., Franks, A.L., 1992. The importance of parental magma composition to calc-alkaline and tholeiitic evolution: evidence from Umnak Island in the Aleutians. J. Geophys. Res., Solid Earth 97, 321–343.
Morris, J., Hart, S., 1983. Isotopic and incompatible element constraints on the genesis of island arc volcanics from Cold Bay and Amak Island, Aleutians, and implications for mantle structure. Geochim. Cosmochim. Acta 47, 2015–2030.
Mullen, E., Weis, D., Marsh, N., Martindale, M., 2017. Primitive arc magma diversity: new geochemical insights in the Cascade Arc. Chem. Geol. 448, 43–70.
Nickel, K., 1986. Phase equilibria in the system SiO2-MgO-Al2O3-CaO-Cr2O3 (SMACCR) and their bearing on spinel/garnet lherzolite relationships. Neues Jahrb. Mineral. Abh. 155, 259–287.
Patino, L.C., Carr, M.J., Feigenson, M.D., 2000. Local and regional variations in Central American arc lavas controlled by variations in subducted sediment input. Contrib. Mineral. Petrol. 138, 265–283.
Pearce, J.A., 1983. Role of the sub-continental lithosphere in magma genesis at active continental margins. In: Hawkesworth, C.J., Norry, M.J. (Eds.), Continental Basalts and Mantle Xenoliths. Shiva, Nantwich, pp. 231–249.
Plank, T., 2005. Constraints from thorium/lanthanum on sediment recycling at subduction zones and the evolution of the continents. J. Petrol. 46, 921–944.
Plank, T., 2013. The chemical composition of subducting sediments. In: The Crust. In: Treatise on Geochemistry, vol. 4.
Plank, T., Cooper, L.B., Manning, C.E., 2009. Emerging geothermometers for estimating slab surface temperatures. Nat. Geosci. 2, 611–615.
Plank, T., Langmuir, C.H., 1988. An evaluation of the global variations in the major element chemistry of arc basalts. Earth Planet. Sci. Lett. 90, 349–370.
Plank, T., Langmuir, C.H., 1993. Tracing trace elements from sediment input to volcanic output at subduction zones. Nature 362, 739–743.
Robinson, J.A.C., Wood, B.J., 1998. The depth of the spinel to garnet transition at the peridotite solidus. Earth Planet. Sci. Lett. 164, 277–284.
Salters, V.J., Longhi, J.E., Bizimis, M., 2002. Near mantle solidus trace element partitioning at pressures up to 3.4 GPa. Geochem. Geophys. Geosyst. 3, 1–23.
Salters, V.J., Stracke, A., 2004. Composition of the depleted mantle. Geochem. Geophys. Geosyst. 5.
Schilling, J., Zajac, M., Evans, R., Johnston, T., White, W., Devine, J., Kingsley, R., 1983. Petrologic and geochemical variations along the Mid-Atlantic Ridge from 29 degrees N to 73 degrees N. Am. J. Sci. 283, 510–586.
Schmidt, M.W., Jagoutz, O., 2017. The global systematics of primitive arc melts. Geochem. Geophys. Geosyst. 18, 2817–2854.
Sisson, T., Kelemen, P., 2018. Near-solidus melts of MORB+ 4 wt% H2O at 0.8–2.8 GPa applied to issues of subduction magmatism and continent formation. Contrib. Mineral. Petrol. 173, 1–23.
Skora, S., Blundy, J., 2010. High-pressure hydrous phase relations of radiolarian clay and implications for the involvement of subducted sediment in arc magmatism. J. Petrol. 51, 2211–2243.
Spandler, C., Mavrogenes, J., Hermann, J., 2007. Experimental constraints on element mobility from subducted sediments using high-P synthetic fluid/melt inclusions. Chem. Geol. 239, 228–249.
Stolper, E., Newman, S., 1994. The role of water in the petrogenesis of Mariana trough magmas. Earth Planet. Sci. Lett. 121, 293–325.
Straub, S.M., Gómez-Tuena, A., Bindeman, I.N., Bolge, L.L., Brandl, P.A., Espinasa-Perena, R., Solari, L., Stuart, F.M., Vannucchi, P., Zellmer, G.F., 2015. Crustal recycling by subduction erosion in the central Mexican Volcanic Belt. Geochim. Cosmochim. Acta 166, 29–52.
Till, C.B., 2017. A review and update of mantle thermobarometry for primitive arc magmas. Am. Mineral. 102, 931–947.
Tormey, D.R., Hickey-Vargas, R., Frey, F.A., López-Escobar, L., 1991. Recent lavas from the Andean volcanic front (33 to 42 S); interpretations of along-arc compositional variations. Spec. Pap., Geol. Soc. Am. 265, 57–78.
Turner, S.J., Langmuir, C.H., 2015a. The global chemical systematics of arc front stratovolcanoes: evaluating the role of crustal processes. Earth Planet. Sci. Lett. 422, 182–193.
Turner, S.J., Langmuir, C.H., 2015b. What processes control the chemical compositions of arc front stratovolcanoes? Geochem. Geophys. Geosyst.
Turner, S.J., Langmuir, C.H., 2022a. An evaluation of five models of arc volcanism. J. Petrol.
Turner, S.J., Langmuir, C.H., 2022b. Sediment and ocean crust both melt at subduction zones. Earth Planet. Sci. Lett. https://doi.org/10.1016/j.epsl.2022.117424.
Turner, S.J., Langmuir, C.H., in preparation. An alternative to the paradigm of 'sediment melts plus slab fluids' for arc magma chemistry.
Turner, S.J., Langmuir, C.H., Dungan, M.A., Escrig, S., 2017. The importance of mantle wedge heterogeneity to subduction zone magmatism and the origin of EM1. Earth Planet. Sci. Lett. 472, 216–228.
Turner, S.J., Langmuir, C.H., Katz, R.F., Dungan, M.A., Escrig, S., 2016. Parental arc magma compositions dominantly controlled by mantle-wedge thermal structure. Nat. Geosci. 9, 772–776.
Valdenegro, P., Muñoz, M., Yáñez, G., Parada, M.A., Morata, D., 2019. A model for thermal gradient and heat flow in central Chile: the role of thermal properties. J. South Am. Earth Sci. 91, 88–101.
van Keken, P.E., Wada, I., Abers, G.A., Hacker, B.R., Wang, K., 2018. Mafic high-pressure rocks are preferentially exhumed from warm subduction settings. Geochem. Geophys. Geosyst. 19, 2934–2961.
Wei, S.S., Wiens, D.A., van Keken, P.E., Cai, C., 2017. Slab temperature controls on the Tonga double seismic zone and slab mantle dehydration. Sci. Adv. 3, e1601755.
White, W.M., 2015. Probing the Earth's deep interior through geochemistry. Geochem. Perspect. 4.
Wieser, P.E., Turner, S.J., Mather, T.A., Pyle, D.M., Savov, I.P., Orozco, G., 2019. New constraints from Central Chile on the origins of enriched continental compositions in thick-crusted arc magmas. Geochim. Cosmochim. Acta 267, 51–74.
Woodhead, J., Eggins, S., Gamble, J., 1993. High field strength and transition element systematics in island arc and back-arc basin basalts: evidence for multi-phase melt extraction and a depleted mantle wedge. Earth Planet. Sci. Lett. 114, 491–504.
Woodhead, J., Hergt, J., Davidson, J., Eggins, S., 2001. Hafnium isotope evidence for 'conservative'element mobility during subduction zone processes. Earth Planet. Sci. Lett. 192, 331–346.
Woodhead, J., Stern, R.J., Pearce, J., Hergt, J., Vervoort, J., 2012. Hf-Nd isotope variation in Mariana Trough basalts: the importance of "ambient mantle" in the interpretation of subduction zone magmas. Geology 40, 539–542.
Workman, R.K., Hart, S.R., 2005. Major and trace element composition of the depleted MORB mantle (DMM). Earth Planet. Sci. Lett. 231, 53–72.
Yao, L., Sun, C., Liang, Y., 2012. A parameterized model for REE distribution between low-Ca pyroxene and basaltic melts with applications to REE partitioning in low-Ca pyroxene along a mantle adiabat and during pyroxenite-derived melt and peridotite interaction. Contrib. Mineral. Petrol. 164, 261–280.
Yogodzinski, G.M., Kelemen, P.B., Hoernle, K., Brown, S.T., Bindeman, I., Vervoort, J.D., Sims, K.W., Portnyagin, M., Werner, R., 2017. Sr and O isotopes in western Aleutian seafloor lavas: implications for the source of fluids and trace element character of arc volcanic rocks. Earth Planet. Sci. Lett. 475, 169–180.